General Disclaimer

One or more of the Following Statements may affect this Document

- This document has been reproduced from the best copy furnished by the organizational source. It is being released in the interest of making available as much information as possible.

- This document may contain data, which exceeds the sheet parameters. It was furnished in this condition by the organizational source and is the best copy available.

- This document may contain tone-on-tone or color graphs, charts and/or pictures, which have been reproduced in black and white.

- This document is paginated as submitted by the original source.

- Portions of this document are not fully legible due to the historical nature of some of the material. However, it is the best reproduction available from the original submission.

Accelerator Irradiations of Minerals: Implications for Track Formation Mechanisms and for Studies of Lunar and Meteoritic Materials.*

M. Seitz, M. C. Wittels, M. Maurette,
and R. M. Walker
Laboratory for Space Physics
Washington University
St. Louis, Missouri 63130

and

H. Heckman
Lawrence Radiation Laboratory
Berkeley, California

*Work supported in part by NAS 9-8165 and McDonnell-Douglas Contract #Z80058T.

SPP-16

May, 1969

ABSTRACT

Natural crystals of feldspars, pyroxenes, quartz and apatite have been irradiated in the Berkeley HILAC with neon and argon ions of up to 10.2 MeV/amu with maximum doses of 1.6×10^{13} argon ions/cm^2 and 4.0×10^{13} neon ions/cm^2 respectively. The samples were thinned to thicknesses near 30 microns, stacked to form the target and then bathed completely in the ion beams. X-ray and optical observations revealed: (a) a crystal distortion and curvature with the argon irradiation similar to that produced in mica; (b) a lesser effect from neon bombardment; (c) a fracturing of the crystal samples which depended on the total dose and energy of the incident ion; (d) polygonized structures produced when either neon or argon ions (with sufficiently high concentration) were trapped within the crystals. The interpretation of the measurements, their correlation with the mechanism of track formation and implications concerning the alteration of the lunar surface due to solar particles and the exposure of lunar and meteoritic material in the ancient solar flare cosmic rays are discussed.

INTRODUCTION

In this preliminary investigation we attempt to characterize the damage produced by relatively high fluxes of artificially accelerated heavy ions in a small group of minerals characteristic of meteorites and which possibly may be found on the lunar surface; we have also included some other minerals like mica in which the registration of heavy ion tracks has been extensively studied. The fluxes of the ions were chosen to simulate exposure time of the minerals in the solar flare cosmic rays ranging from 0.5 to 10 x 10^6 years. An extended paper in preparation will dwell in more detail on the experimental techniques, the effects observed and the applications of the results to lunar and meteoritic materials.

The main purposes of this study are: (a) to identify the radiation effects produced in lunar or meteoritic materials exposed to high fluxes of solar flare cosmic rays, (b) to utilize these effects for dosimetry purposes; (c) to determine whether such high flux exposures could produce important physical changes on the surface of atmosphere-free and magnetic field-free bodies like the Moon.

EXPERIMENTAL PROCEDURE AND RESULTS

Thin discs (~30μ) of natural single crystals of feldspars, pyroxene, quartz, apatite, mica and olivine were irradiated in the Berkeley HILAC with neon and argon ions having an energy of 10.2 MeV/amu, with maximum doses of 4.0 x 10^{13} neon/cm^2 and 1.6 x 10^{13} argon/cm^2. Irradiations were also made in the Washington University cyclotron with α particles of 30 MeV, up to doses of 10^{16} α/cm^2. Before hitting some of the targets the ions were slowed down to obtain information on the energy variation of damage. The techniques used to prepare and irradiate the samples are described in detail elsewhere(1).

Following the irradiation, we observed by optical and stereo-scan electron microscopy that fracturing has occurred in some of the discs (figure 1). This fracturing depends on the total dose and energy of the inciden ions as well as the type of mineral and irradiating ion. The size of the fragments ranged from 1000 microns down to ~10 microns, starting with discs of 3 mm in diamter. Some of the discs which did not fracture, as well as the fragmented samples, showed a curvature easily visible with the unaided eye.

The minerals investigated here may be readily classified according to their sensitivity to be distorted. Such a classification* is reported on Table 1 (it does not include the results observed when the ions stopped in the samples): (a) the most sensitive minerals are albite, quartz, apatite which are distorted by the neon irradiation; (b) the intermediate sensitivity group includes all the remaining minerals except olivine. All these minerals were visibly distorted only by the argon irradiation; (c) the least sensitive crystal was olivine which showed no

*A more complete classification, including irradiation with proton, α particles, oxygen ions and fission fragments will be found in reference 1.

measurable effects when irradiated with argon ions. In each group the minerals were arranged according to the magnitude of the induced curvature for a given energy flux.

In an attempt to better understand the fracturing process and to correlate it with lattice distortions, Laue x-ray transmission patterns and precession diffraction patterns were taken of the irradiated samples.

The Laue transmission photographs in general showed a radial elongation (asterism) of the diffraction maxima (figure 2). Although the sensitivity to a particular ion is different for each mineral the asterism was produced by the microscopic curvature of the crystal as verified in more detail for mica(2). The curvature increased either with an increase in flux or with a decrease in the energy of the ions and could be measured optically as well as with x-ray diffraction methods.

The structure of some of the strongly distorted crystals was investigated in more detail by means of the x-ray precession method. It was found that although microscopic distortion was present, the microscopic crystal structure was not greatly altered. This can be seen in the reciprocal lattice photographs in figure 3: zero and upper level photography revealed no change in space group symmetry, and lattice parameter shifts greater than 0.1% were not detected.

Thermal isochronal annealing experiments were then performed on some irradiated samples in which the bombarding ions were not stopped. It was found that if the curvature was not too severe a recovery to the original non-distorted state occured. Furthermore the annealing of the distortion as examined through the Laue asterism recovery was closely related with the recovery of fission fragment tracks as illustrated on figure 4 where we have plotted the normalized length of the asterism and the normalized track density versus the annealing temperature. Annealing experiments were performed in diopside, mica, albite, orthoclase and enstatite with similar results.

Polygonized structures resulted when sufficiently large concentrations of argon or neon were trapped in the crystals as shown in figure 5. This figure shows the Laue transmission photograph of an enstatite disc in which the argon beam was stopped. The appearance of numerous small discrete diffraction maxima instead of the normal Laue spots, reveals the presence of closely aligned crystallites as small as one micron. This effect is probably not due to radiation damage but to a gas trapping mechanism. It was observed with the lowest flux of particles we used; for example 10^{15} α/cm^2 in mica.

DISCUSSION OF THE RESULTS

Remarks on the Radiation Damage Mechanism

It has been suggested[3] that there is a critical rate of primary ionization for the registration of heavy ion tracks in which only the ions whose primary rate of ionization are greater than the critical value, Jc, can produce etchable tracks. The existence of such a threshold can be explained in two different ways: (a) as J becomes smaller than Jc, the concentration in defects along the path of the ion is suddenly decreased; the threshold then would be a characteristic of the radiation damage mechanism; (b) the defects are still produced when $J < Jc$ but the separation between consecutive islands of damage becomes too large to allow a fast continuous etching of the track; in this case, a primary "track" is still formed but cannot be etched, the observed threshold is then characteristic of the process used to reveal the tracks.

It seems to us that this second explanation is supported: (a) by our annealing experiments of neon irradiated silicates which indicate that track like defect structure exist in solids bombarded with ions with $J < Jc$. (b) by the work of Lambert et al[4] showing that no drastic decrease in the concentration of defects occurs for argon ions in mica when $J < Jc$.

Implications for Lunar and Meteoritic Minerals

A small grain of silicate material in space is exposed to a variety of particle irradiations ranging from low energy solar wind particles (~1 KeV/amu) to galactic cosmic rays (1 GeV/amu). Samples that are ~100μ in size will be most affected by the abundant solar cosmic rays whose energies are comparable to those used in this experiment. From our results, we are led to the following conclusions concerning solar cosmic ray effects:

1. The most easily observable gross radiation damage effect produced is a distortion of the normal Laue diffraction pattern. An irradiation time of 10^6 years would be easily measurable. We should note here, however, that the effects we have observed are all produced by parallel beams of particles. There is the possibility that an isotropic irradiation would give a much smaller effect.
2. The effects of a 10^6 year exposure on the long range lattice disorder of silicate crystals is so small as to be unmeasurable by our techniques.
3. In spite of their low abundance, the medium and heavy components of the solar cosmic rays produce more damage than the vastly more abundant light nuclei such as hydrogen and helium. In simulating solar flare effects it is therefore essential to include heavy ion irradiations.
4. The most striking effects were produced by particles that actually stopped in the targets. From this observation we believe that it is quite possible that the trapped gas component may be more important in

producing observable physical effects than the direct radiation damage produced by the passage of nuclear particles through the sample.

The cracking and fragmentation that we observed in certain samples suggests that solar flare cosmic rays might conceivalby play a role in surface erosion processes on the moon. The Surveyor photographs have shown that many surface rocks are rounded as if they were being subjected to a continual wearing away. The lunar surface is also known to be covered with a layer of very fine material. Although the dominant erosion process is likely to be due to micrometeorite infall, solar cosmic rays may also produce measurable erosion effects, probably due mostly to the effects of trapped gas.

An interesting application of the results in this paper can be made to the study of the Kapoeta gas rich achondrite. Recently Pellas et al[5] and Lal et al[6] have reported the exciting observation, based on fossil track studies, that individual grains in this meteorite have been subjected to solar irradiations prior to their incorporation in the meteorite. Pellas et al[5] also have observed an x-ray distortion of the Kapoeta crystals which they attributed to radiation damage effects.

We have confirmed the observation of x-ray distortions in Kapoeta (figure 6), but believe it unlikely that the distortion was produced by radiation damage.

The flux of iron group nuclei estimated from the track studies of Pellas et al[5] ~10^9 ions/cm^2. Our x-ray studies of silicate minerals irradiated with argon ions and those of Wittels and Sherrill[7] and Romieu and Bloch[8] with silicate minerals exposed to fission fragments show that measurable x-ray distortion appears for fluxes of heavy ion several orders of magnitude higher (>10^{11} ions/cm^2).

Our conclusion is further supported by annealing experiments: if the distortion was due to radiation damage, we could expect to observe its thermal recovery at a temperature ~500°C corresponding to the annealing of heavy ion tracks in orthopyroxene crystals. We performed such an annealing experiment and observed no recovery of the distortion up to the highest temperature (700°) we used.

The origin of the distortion remains to be found. It could be due to the rare gas trapped in the lattice of the minerals and therefore could still be related to a solar flare irradiation of the crystals. It is also possible that the distortion is a manifestation of a mechanical effect such as a shock event, and is essentially unrelated to the radiation history.

We look forward with anticipation to the reception of returned lunar samples to investigate the effects of irradiations of the type we have been discussing here in nature.

BIBLIOGRAPHY

1. M. Seitz, M. C. Wittels, M. Maurette, R. M. Walker H. Heckman, Radiation Damage and Gas Trapping Effects in Minerals: Application to Lunar and Meteoritic Studies, to be submitted to J. Geophys. Res.

2. M. Seitz, M. Maurette, H. Heckman, Heavy Ion Radiation Damage in Mica, Bull. Am. Phys. Soc. 13, 1393 (1968).

3. R. L. Fleisher, P. B. Price, R. M. Walker, E. L. Hubbard, Criterion for Registration in Dielectric Track Detectors, Phys. Rev. 156, 353 (1967).

4. M. Lambert, A. M. Levelut, Etude par Diffusion des Rayons x aux Petis Angles, de Mica Muscovite Irradie par des Ions d'Argon, International Topical Conference on Nuclear Track Registration in Insulating Solids and Applications, Clermand-Fernand.

5. P. Pellas, G. Poupeau, J. C. Lorin H. Reeves, J. Audouze, Primitive Low-Energy Particle Irradiation of Meteoritic Crystals: (a) preprint, to be submitted to Nature; (b) Trans. Am. Geophys. Union 50, 222 (1969).

6. D. Lal, R. S. Rajan, Observations Relating to Space Irradiation of Individual Crystals of Gas Rich Meteorites, preprint, to be submitted to Nature.

7. M. C. Wittels, F. A. Sherrill, Some Irradiation Effects in Nonmetallic Crystals. Advances in X-Ray Analysis, V. 3, 269 (195-

8. M. Romieu, J. Bloch, Amorphisation du Mica Muscovite par Irradiation aux Fragments de Fission, C. R. Acad. Sc. Paris 260, 4194 (1965).

TABLE 1

Sensitivity Scale of Minerals

MINERALS	SENSITIVITY	X-RAYS OBSERVATIONS
Olivine	Least Sensitive	No distortion with 1.6×10^{13} argon/cm^2
Hypersthene Diopside Enstatite Labradorite Mica Orthoclase	Moderately Sensitive	Distortion with 1.6×10^{13} argon/cm^2 but not with 4.0×10^{13} Neon/cm^2
Quartz Albite Apatite	Most Sensitive	Distortion with 4.0×10^{13} Neon/cm^2

Fig. 1 Fractured crystals from exposure to 16x 10^{12} argon ions/ cm^2.

First photograph: Quartz as seen in the irradiation holder, 17x.

Second photograph: Topaz, 17x.

Fig. 2 Laue photograph of diopside before and after receiving $16x10^{12}$ argon ions/cm^2 at 5 mev/AMU.

Fig. 3 Precession photographs of enstatite, $a^* - c^*$ projection. Non-irradiated and irradiated with $16x10^{12}$ argon ions/cm^2 at 8mev/AMU. No differences in lattice structure or lattice parameters can be seen in photographs like these.

Fig. 4 Plot of the normalized distortion, as measured by the elongation of the diffraction spots verses the annealing temperature. Also plotted is the normalized fission track density verses the annealing temperature. The crystals were annealed for 2 hours at each temperature.

Fig. 5 Laue photographs of enstatite, normal non-irradiated crystal and one in which the beam of $16x10^{12}$ argon ions/cm^2 has stopped.

Fig. 6 Enstatite crystal from Kapoeta, Laue photograph before and after annealing the crystal at 700° C. for 2 hours.

Fig. 2

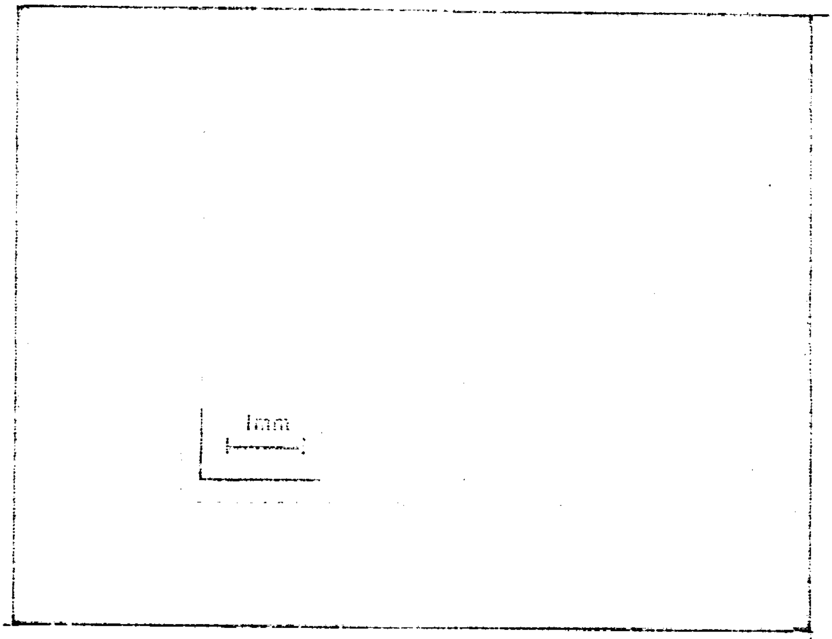

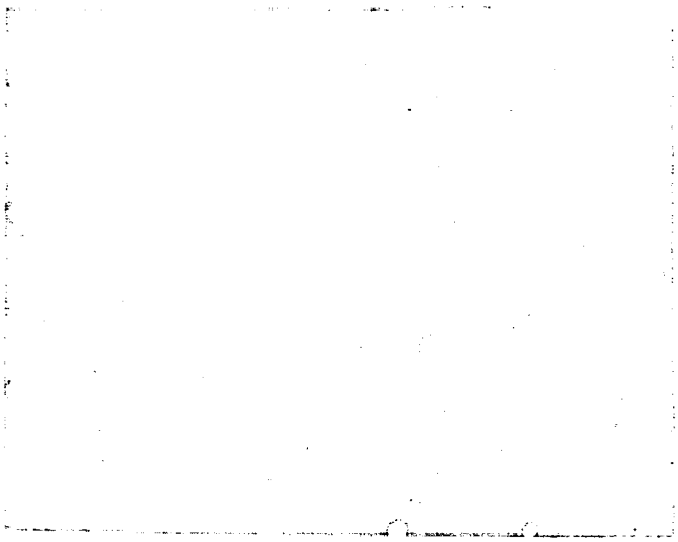

Fig 6

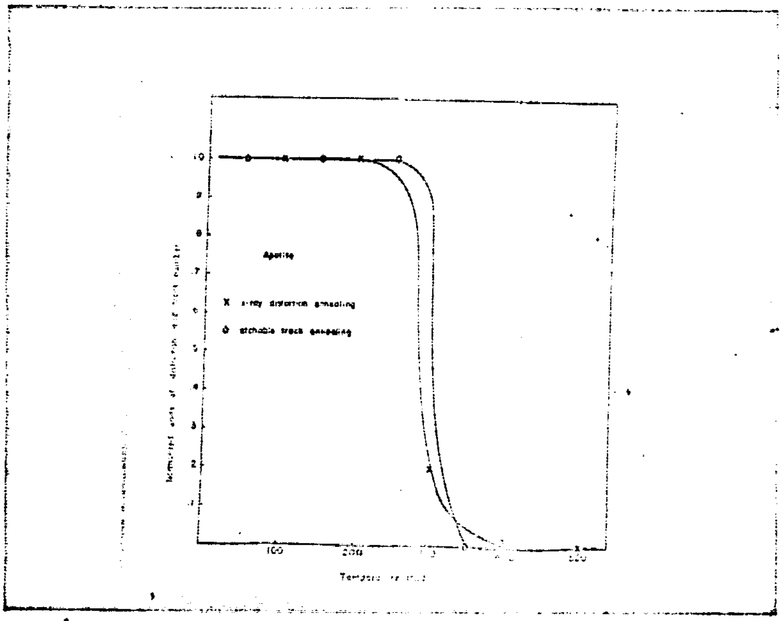

Apatite
X x-ray distortion annealing
O etchable track annealing
1.0
100
200

Fig. 6